INFECTION AND IMMUNITY, Nov. 2011, p. 4353–4360 Vol. 79, No. 11
0019-9567/11/$12.00 doi:10.1128/IAI.05677-11

Clostridium perfringens Iota-Toxin b Induces Rapid Cell Necrosis[▽]

Masahiro Nagahama,[1]* Mariko Umezaki,[1] Masataka Oda,[1] Keiko Kobayashi,[1] Shigenobu Tone,[2] Taiji Suda,[3] Kazumi Ishidoh,[4] and Jun Sakurai[1]

Department of Microbiology, Faculty of Pharmaceutical Sciences, Tokushima Bunri University, Yamashiro-cho, Tokushima 770-8514, Japan[1]; Department of Biochemistry, Kawasaki Medical School, 577 Matsushima, Kurashiki, Okayama 701-0192, Japan[2]; Electron Microscope Center, Kawasaki Medical School, 577 Matsushima, Kurashiki, Okayama 701-0192, Japan[3]; and Division of Molecular Biology, Institute for Health Sciences, Tokushima Bunri University, Yamashiro-cho, Tokushima 770-8514, Japan[4]

Received 16 July 2011/Returned for modification 5 August 2011/Accepted 30 August 2011

***Clostridium perfringens* iota-toxin is a binary toxin composed of an enzyme component (Ia) and a binding component (Ib). Each component alone lacks toxic activity, but together they produce cytotoxic effects. We examined the cytotoxicity of iota-toxin Ib in eight cell lines. A431 and A549 cells were susceptible to Ib, but MDCK, Vero, CHO, Caco-2, HT-29, and DLD-1 cells were not. Ib bound and formed oligomers in the membranes of A431 and MDCK cells. However, Ib entered MDCK cells but not A431 cells, suggesting that uptake is essential for cellular survival. Ib also induced cell swelling and the rapid depletion of cellular ATP in A431 and A549 cells but not the insensitive cell lines. In A431 cells, Ib binds and oligomerizes mainly in nonlipid rafts in the membranes. Disruption of lipid rafts by methyl-β-cyclodextrin did not impair ATP depletion or cell death caused by Ib. Ib induced permeabilization by propidium iodide without DNA fragmentation in A431 cells. Ultrastructural studies revealed that A431 cells undergo necrosis after treatment with Ib. Ib caused a disruption of mitochondrial permeability and the release of cytochrome *c*. Staining with active-form-specific antibodies showed that the proapoptotic Bcl-2-family proteins Bax and Bak were activated and colocalized with mitochondria in Ib-treated A431 cells. We demonstrate that Ib by itself produces cytotoxic activity through necrosis.**

Clostridium perfringens type E, which produces an iota-toxin consisting of an enzyme component (Ia) and a binding component (Ib), causes antibiotic-associated enterotoxemia in calves and lambs (18, 23). Ib binds to a receptor and transfers Ia into the cytosol, where Ia ADP-ribosylates actin. Each component lacks toxic activity alone, but together they act in binary combinations to produce cytotoxic, lethal, and dermonecrotic activities (3, 17). Iota-toxin belongs to a family of binary actin-ADP-ribosylating toxins that includes *Clostridium botulinum* C2 toxin, *Clostridium spiroforme* iota-like toxin, *Clostridium difficile* ADP-ribosyltransferase, and vegetative insecticidal protein (VIP) from *Bacillus cereus* (3).

Ia ADP-ribosylates skeletal muscle α-actin and nonmuscle β/γ-actin (2). Crystallography of Ia complexed with NADPH and site-directed mutagenesis revealed that it is divided into two domains, the N domain (residues 1 to 210), which is responsible for interaction with Ib, and the C domain (residues 211 to 423), which is involved in the catalytic activity of ADP-ribosyltransferase (19, 27). Furthermore, we reported the structure of a Michaelis complex with Ia, actin, and a nonhydrolyzable NAD^+ analogue (28). Based on this structure, we revealed that Glu-378 on the EXE loop of Ia is in close proximity to Arg-177 in actin, and we proposed that the ADP-ribosylation of Arg-177 proceeds by an SN1 reaction (28).

Ib binds to cells, forming oligomers to create ion-permeable channels (4, 11, 25). Iota-toxin enters host cells and induces toxicity by exploiting the cell's endogenous pathways as follows (3–5, 20). Through its C-terminal part, Ib recognizes distinct, though as-yet-unidentified, receptors on the cell surface, a membrane protein sensitive to pronase (24). Ib specifically binds to a receptor on the cytoplasmic membrane of cells and accumulates in lipid rafts, and the Ia bound to the oligomers formed on the rafts then enters the cell (6, 13). Ia and Ib are transported to the early endosome, where acidification promotes cytosolic entry of Ia (6, 13). Then Ia binds to G-actin in the cytosol and ADP-ribosylates it, thereby blocking the polymerization of actin and eventually intoxicating cells (4, 20).

Ib displays significant homology with the protective antigen (PA) of anthrax toxins (54.4% similarity overall) and C2II (39.0%), suggesting that they have similar modes of action (3, 14). PA (15) and C2II (3) bound to cell surface receptors and interacted with the enzyme components edema factor and lethal factor for PA and C2I for C2II, respectively, mediating their entry into target cells. The crystal structure of PA and C2II reveals four domains (15, 21). The N and C termini in the binding component, designated domain I and domain IV, respectively, represent the docking site for the enzyme component and the binding site for the cells. We reported that the conserved Ca^{2+}-binding motif in the N-terminal region of Ib plays a role in the interaction of Ib with Ia in the presence of Ca^{2+} (9).

Marvaud et al. and Stiles et al. (10, 24) reported that Ib strongly binds to the cell surface receptor of Vero and MDCK cells, which are sensitive to iota toxin, but not that of FRHL-103 and MRC-5 cells, which are highly resistant to the toxin. Knapp et al. (8) reported that Ib forms cation-permeable chan-

* Corresponding author. Mailing address: Department of Microbiology, Faculty of Pharmaceutical Sciences, Tokushima Bunri University, Yamashiro-cho, Tokushima 770-8514, Japan. Phone: 81-088-622-9611. Fax: 81-088-655-3051. E-mail: nagahama@ph.bunri-u.ac.jp.

▽ Published ahead of print on 12 September 2011.

nels in artificial lipid membranes. We revealed that the Ib-induced release of K^+ from the cells is dependent on the formation of oligomers by Ib in Vero cells, but the oligomers do not induce cytotoxicity (11). We cannot explain why the formation of an oligomer does not lead to cytotoxicity. Furthermore, little is known about the biological activity of Ib. Here, we investigated the cytotoxic activity of Ib in six cell lines and identified two sensitive cell lines. The results indicate that Ib induces rapid necrosis among the sensitive cells.

MATERIALS AND METHODS

Materials. Recombinant Ib was expressed, fused with glutathione *S*-transferase (GST), in *Escherichia coli* BL21, as described previously (11). Rabbit anti-Ib antibody was prepared as described previously (17). Methyl-β-cyclodextrin (MbCD), Z-VAD-FMK, staurosporine, propidium iodide (PI), ethidium bromide, 3-methyladenine, and a protease inhibitor mixture were obtained from Sigma (St. Louis, MO). Mouse anti-caveolin-1, anti-Lyn, and anti-β-actin antibodies were purchased from Santa Cruz Biotechnology (Santa Cruz, CA). Horseradish peroxidase-labeled goat anti-rabbit immunoglobulin G (IgG), horseradish peroxidase-labeled sheep anti-mouse IgG, and an enhanced chemiluminescence (ECL) Western blotting kit were purchased from GE Healthcare (Tokyo, Japan). Dulbecco's modified Eagle's medium (DMEM) and Hanks' balanced salt solution (HBSS) were obtained from Gibco BRL (New York, NY). Mouse anti-cytochrome *c* antibody (6H2.B4) was purchased from BD Bioscience (Tokyo, Japan). Alexa Fluor 568-conjugated goat anti-rabbit IgG, Alexa Fluor 568-conjugated goat anti-mouse IgG, MitoTracker red CMXRos, Cellular Lights Mito-GFP BacMam 1.0, Hoechst 33342, and 4′,6′-diamino-2-phenylindole (DAPI) were provided by Molecular Probes (Eugene, OR). Rabbit anti-Bax-NT and anti-Bak-NT antibodies were purchased from Millipore (Tokyo, Japan). Rabbit anti-active caspase 3 antibody was obtained from Promega (Tokyo, Japan). All other chemicals were of the highest grade available from commercial sources.

Cell culture. Human epithelial carcinoma cells (A431), human lung adenocarcinoma cells (A549), human colon epithelial carcinoma cells (DLD-1), human colon carcinoma cells (Caco-2), African green monkey kidney cells (Vero), Madin-Darby canine kidney cells (MDCK), and Chinese hamster ovary cells (CHO) were obtained from Riken Cell Bank (Tsukuba, Japan). Human colon adenocarcinoma cells (HT-29) were purchased from DS Pharma Biomedical (Osaka, Japan). They were cultured in DMEM supplemented with 10% fetal calf serum (FCS), 100 U/ml of penicillin, 100 μg/ml of streptomycin, and 2 mM glutamine (FCS-DMEM). All incubation steps were carried out at 37°C in a 5% CO_2 atmosphere.

Cell viability. Cell viability was determined by the MTS (3-(4,5-dimethylthiazol-2-yl)-5-(3-carboxymethoxyphenyl)-2-(4-sulfophenyl)-2*H*-tetrazolium; Promega) inner salt conversion assay (MTS assay). The absorbance was read at 490 nm using an enzyme-linked immunosorbent assay plate reader. Cell viability was calculated as mean absorbance of the toxin group divided by that of the control (12). In some experiments, heat-inactivated Ib was prepared by heating at 95°C for 10 min.

Measurement of ATP. Cellular ATP content was measured using a luminescence assay (Cell-Titer Glo kit; Promega) following the manufacturer's instructions. Briefly, cells were incubated with Ib at 37°C for specific periods. Final luminescence was measured in a TopCount NXT microplate luminescence counter (Perkin-Elmer, Waltham, MA).

Sucrose gradient fractionation. The separation of lipid rafts was carried out by flotation-centrifugation on a sucrose gradient (12, 13). A431 cells were plated in 100-mm-diameter tissue culture dishes 24 h before use. Ib was added to cells in FCS-DMEM at 4°C for 1 h. The cells were washed and transferred into warmed FCS-DMEM (37°C) for 1 h. They were then rinsed with Hanks balanced salt solution (HBSS) and lysed by exposure to 1% Triton X-100 at 4°C for 30 min in HBSS containing the protease inhibitor mixture. The lysate was scraped from the dishes with a cell scraper and homogenized by passage through a 22-gauge needle. The lysate was adjusted to contain 40% sucrose (wt/vol), overlaid with 2.4 ml of 36% sucrose and 1.2 ml of 5% sucrose in HBSS, centrifuged at 45,000 rpm (250,000 × *g*) for 18 h at 4°C in an SW55 rotor (Beckman Instruments, Inc., Palo Alto, CA), and fractionated from the top (0.4 ml/fraction). The aliquots were subjected to sodium dodecyl sulfate-polyacrylamide gel electrophoresis (SDS-PAGE). Ib was detected by Western blotting as described for the immunoblot analysis. Cholesterol contents were assayed spectrophotometrically using a diagnostic kit (Cholesterol C-Test; Wako Pure Chemical, Osaka, Japan).

Immunoblot analysis. The samples were heated in 2% SDS sample buffer at 95°C for 3 min, subjected to SDS-PAGE, and transferred to a polyvinylidene difluoride membrane (Immobilon P; Millipore). The membrane was blocked with Tris-buffered saline (TBS) containing 2% Tween 20 and 5% skim milk and incubated first with the primary antibody against Ib, caveolin-1, or active caspase 3 in TBS containing 1% skim milk, then with a horseradish peroxidase-conjugated secondary antibody, and finally with an enhanced chemiluminescence analysis kit (GE Healthcare).

Influx of propidium iodide. A431 cells on 96-well plates were incubated with or without Ib and with propidium iodide (PI; 5 μg/ml) at 37°C. Then, the plates were read with a spectrofluorimeter (Tecan, Tokyo, Japan) (excitation, 380 nm; emission, 620 nm). The results were expressed as the percentage of fluorescence obtained compared to nonintoxicated cells incubated with 0.5% Triton X-100 at 37°C.

DNA gel electrophoresis. A431 cells grown in 3.5-cm dishes were incubated without or with Ib (250 ng/ml) at 37°C for various periods. DNA was extracted using SepaGene (Sanko-Junyaku, Tokyo, Japan) according to the manufacturer's instructions, and 2 μg of DNA was then subjected to agarose gel electrophoresis (1.5%), followed by ethidium bromide staining. Molecular weight standards were from Takara-Bio (Shiga, Japan). As a positive control of DNA fragmentation, A431 cells were incubated with staurosporine (10 nM) for 24 h and subjected to gel electrophoresis.

Electron microscopy. A431 cells incubated with or without Ib were fixed in 2.5% glutaraldehyde in 0.1 M cacodylate buffer (pH 7.2). After being washed in the same buffer and fixed in 1% OsO_4 for 1 h, the specimens were washed again, dehydrated in an ethanol series, and embedded in Epon 812. Thin sections were cut with a Leica Ultracut UCT microtome, poststained with 2% uranyl acetate and Reynolds lead citrate, and examined using a JEOL JEM-2000EX operated at 80 kV as described previously (26).

Immunofluorescence studies. Cells were plated on a polylysine-coated glass-bottomed dish (Matsunami, Osaka, Japan) and incubated at 37°C in a 5% CO_2 incubator overnight in FCS-DMEM. To study the internalization of Ib, Ib (1 μg/ml) was incubated with cells at 4°C for 1 h in FCS-DMEM. After three washes in cold FCS-DMEM, cells were transferred to FCS-DMEM or FCS-DMEM containing Ia (1 μg/ml) prewarmed to 37°C and incubated at the same temperature for 30 min. They were washed four times with cold phosphate-buffered saline (PBS) and fixed with 4% paraformaldehyde at room temperature. For antibody labeling, the dishes were then incubated at room temperature for 15 min in 50 mM NH_4Cl in PBS and in PBS containing 0.1% Triton X-100 at room temperature for 20 min. After being washed with PBS containing 0.02% Triton X-100, the dishes were incubated at room temperature for 1 h with PBS containing 4% BSA, followed by primary antibody (rabbit anti-Ib antibody) in PBS containing 4% BSA at room temperature for 1 h. They were then washed with PBS containing 0.02% Triton X-100, incubated with secondary antibody (Alexa Fluor 568-conjugated anti-rabbit IgG) in PBS containing 4% BSA at room temperature for 1 h, washed extensively with PBS containing 0.02% Triton X-100, and analyzed under a Nikon A1 laser scanning confocal microscope (Tokyo, Japan). Nuclei were stained with DAPI.

To study the activation of Bax and Bak and release of cytochrome *c*, A431 cells were seeded and grown at 37°C for 12 h on glass-bottomed dishes before transfection with Cellular Lights Mitochondria-GFP BacMam 1.0 according to the manufacturer's instructions; 24 h later, they were treated with Ib, fixed, permeabilized, and blocked as described above. Cells were incubated with active-form-specific anti-Bax, active-form-specific anti-Bak, or anti-cytochrome *c* antibodies and then with species-specific Alexa Fluor 488-conjugated secondary antibodies.

For experiments with MitoTracker red CMXRos, A431 cells were incubated with MitoTracker red CMXRos (200 nM) and Hoechst 33342 (20 μg/ml) at 37°C for 30 min before live cell imaging. All images represent a single section through the focal plane. Images shown in the figures are representative of at least three independent experiments and were produced with Adobe Photoshop v7.0.

RESULTS

Cytotoxicity of Ib. It has been reported that Ib alone has no effect on living cells (3). To investigate the cytotoxicity of Ib, the MTS assay was performed with a variety of cell types. As shown in Fig. 1A, Ib caused death of A431 and A549 cells. A431 cells were more sensitive to Ib than A549 cells. Ib did not induce the death of Vero, MDCK, CHO, Caco-2, HT-29, or DLD-1 cells. Cell viability was also assessed using ATP measurements (Fig. 1B and C). Ib caused a rapid dose- and time-

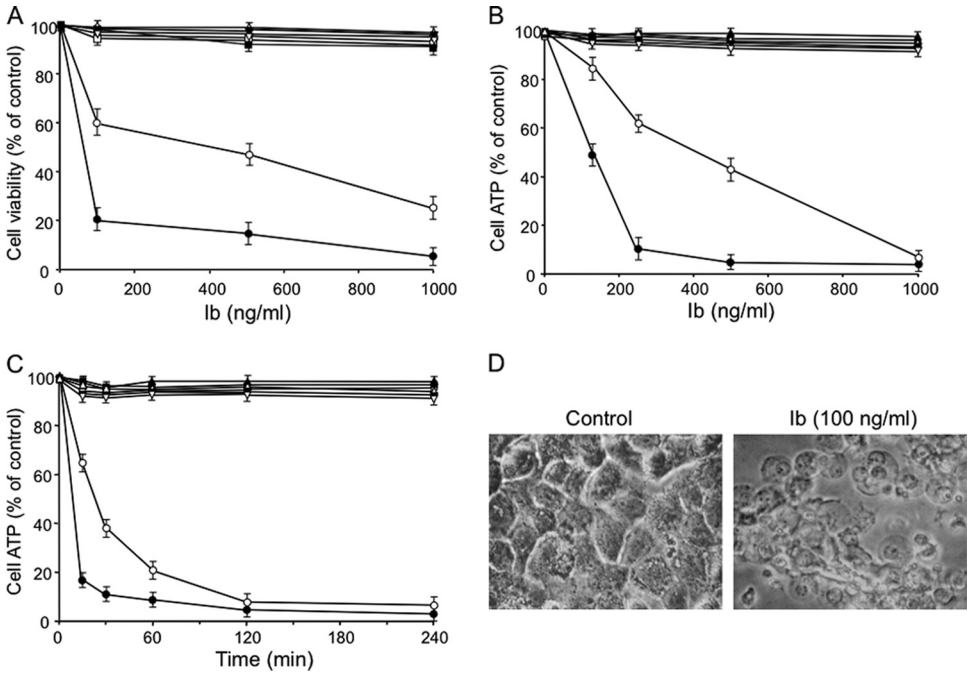

FIG. 1. Cytotoxicity and ATP depletion induced by Ib. (A) Cells were treated with various amounts of Ib at 37°C for 4 h. Cell viability was determined via an assay with MTS, and the number of live cells is shown as a percentage of the value for untreated controls. (B) Cells were incubated with various amounts of Ib at 37°C for 4 h before ATP was measured. (C) Cells were incubated with Ib (250 ng/ml) at 37°C for the periods indicated before ATP was measured. Data are reported as percentages of the values obtained with untreated controls (means ± standard deviations for four independent experiments). Symbols (A, B, and C): ●, A431; ○, A549; ■, MDCK; □, Vero; △, DLD-1; ▲, CHO; ▽, HT-29; ▼, Caco-2. (D) Morphological changes of A431 cells upon treatment with Ib. A431 cells were cultured without or with Ib (250 ng/ml) at 37°C for 4 h. The cells were observed by phase-contrast microscopy. Magnification, ×150.

dependent decrease in the ATP content of A431 and A549 cells, with an almost complete depletion 30 to 60 min after its addition. Ib did not induce any depletion of ATP in the other cells, which were not susceptible to Ib in cytotoxicity assays. The morphological changes induced by Ib in A431 cells are shown in Fig. 1D. The cells showed marked swelling but no blebs. Similar results were obtained with A549 cells (data not shown). Ib had no morphological effect on Ib-insensitive cells (data not shown). No cytotoxicity or ATP depletion was evoked by heat-inactivated Ib, and the cell death and ATP depletion induced by Ib were completely neutralized by an anti-Ib antibody (data not shown). These findings indicated that Ib causes the death of A431 and A549 cells and also induces rapid depletion of cellular ATP.

Binding and internalization of Ib into cells. We reported that Ib binds to Vero cells, forming an oligomer itself to create ion-permeable channels (11). To test the binding and oligomerization of Ib on Ib-sensitive (A431) and -insensitive (MDCK) cells, the cells (5×10^5) were preincubated with Ib in DMEM–10% FCS at 4°C for 60 min, washed, and incubated in the same medium at 37°C for various periods. The treated cells were dissolved in SDS sample solution and analyzed by SDS–7.5% PAGE without heating at 95°C. Ib was analyzed by Western blotting with anti-Ib antibody (Fig. 2A). When the A431 or MDCK cells were incubated with Ib at 4°C for 60 min, only the Ib monomer (76 kDa) was detected. On the other hand, when both cells were incubated with Ib at 37°C, levels of the Ib monomer decreased and Ib oligomer increased in a time-dependent manner, as reported previously (11). As shown in Fig. 2A, the binding of Ib to A431 cells was greater than that to MDCK cells. The data indicated that Ib forms oligomers in Ib-sensitive (A431) and -insensitive (MDCK) cells.

Husmann et al. (7) reported that *Staphylococcus aureus* alpha-toxin, an archetype of bacterial pore-forming toxins, enters a particular cell type and that uptake of the toxin is essential for cellular survival. We investigated the internalization of Ib into A431 and MDCK cells. After the loading of both cells with Ib at 4°C, binding to the plasma membrane was readily detected by confocal immunofluorescence microscopy (Fig. 2B, panel b). When Ib-treated MDCK cells were incubated at 37°C for 30 min, Ib was present in cytoplasmic vesicles (Fig. 2B, panel c). On the other hand, the persistence of Ib on the membrane of A431 cells was confirmed at 37°C (Fig. 2B, panel c). Furthermore, when A431 cells were incubated with Ia plus Ib at 37°C, Ib was also detected in the plasma membrane (Fig. 2B, panel d). The results demonstrate that the ability of a cell type to survive membrane pore formation by Ib appears to depend on its ability to internalize Ib.

We had reported that Ib binds to a receptor on membranes and then moves to lipid rafts and that the Ia bound to Ib in the lipid rafts is internalized in MDCK cells (13). To investigate the binding of Ib to lipid rafts of A431 cells, Ib was incubated with A431 cells in DMEM–10% FCS at 4°C for 60 min, and the cells were treated with 1% Triton X-100 at 4°C for 60 min. The membranes treated with Triton X-100 were fractionated by sucrose density gradient centrifugation. The fractions were subjected to SDS-PAGE and Western blotting using anti-Ib antibody. As shown in Fig. 3A, the Ib monomer (75 kDa) was

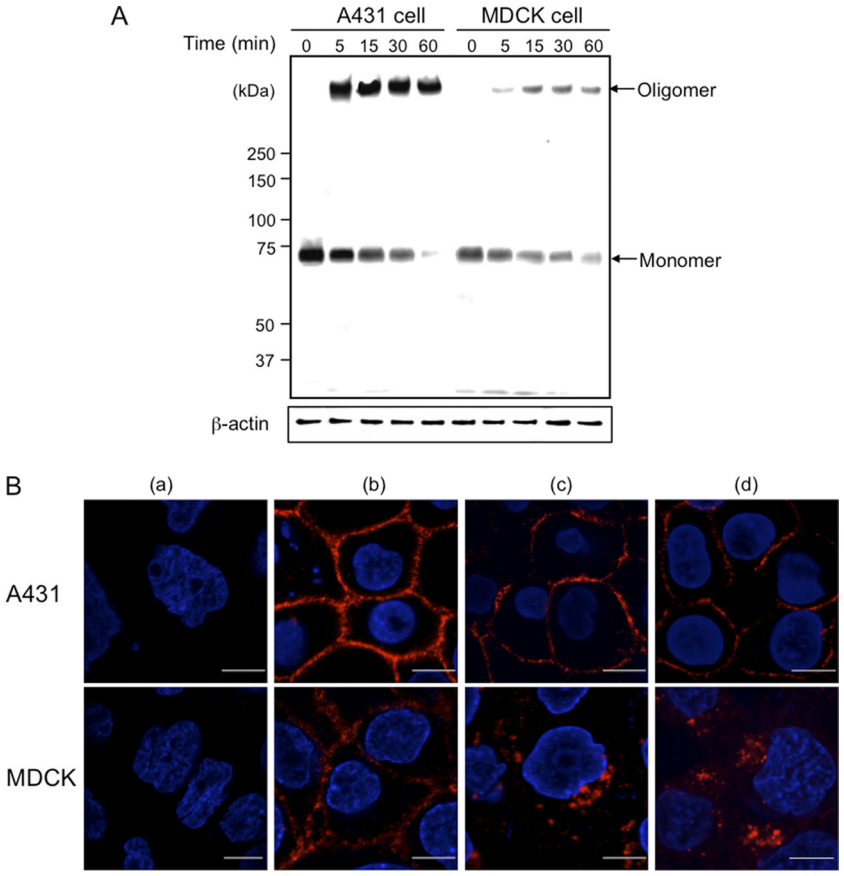

FIG. 2. Binding and formation of oligomers by Ib in A431 cells and MDCK cells. (A) Cells (1×10^6/well) were incubated with Ib (1 μg/ml) at 4°C for 1 h. The cells were rinsed, incubated at 37°C for the period indicated, and subjected to Western blot analyses of Ib and β-actin (control). A typical result from one of three experiments is shown. (B) Binding and internalization of Ib in A431 cells and MDCK cells. Cells were treated without (a) or with (b) Ib (1 μg/ml) at 4°C for 1 h. After washing, cells were incubated with medium only (c) or with medium containing Ia (d) at 37°C for 30 min. Cells were fixed, permeabilized, and stained with anti-Ib antibody and DAPI. Ib (red) and nucleus (blue) were viewed with a confocal microscope. The experiments were repeated three times, and a representative result is shown. Bar, 5 μm.

found in the soluble fractions (fractions 6 to 9). When A431 cells preincubated with Ib at 4°C for 60 min were incubated at 37°C for 30 min, the Triton X-100-soluble fractions (fractions 6 to 9) showed two bands, a minor band corresponding to the Ib monomer and a major band of about 500 kDa, which was reported to be heptameric Ib (11) (Fig. 3B). The monomer and oligomer of Ib were detected in the detergent-insoluble fractions. Caveolin-1 was detected in the insoluble fractions (fractions 2 to 4), where >85% of the cholesterol was detected (Fig. 3C and D), showing that fractions 2 to 4 are lipid rafts. The result suggests that Ib forms an oligomer in the nonlipid rafts of the plasma membranes of A431 cells at 37°C after the binding of the monomer to membranes. Incubating the cells with 10 mM MbCD, an efficient drug that extracts cholesterol from membranes, did not alter the ATP content of untreated cells and had no protective action against the rapid decrease in cellular ATP caused by Ib (data not shown). Consistent with these results, MbCD (10 mM) was found to have no protective effect on cell viability after Ib was added (data not shown). These findings demonstrate that removing cholesterol from lipid rafts is not sufficient to protect cells against the rapid injury caused by Ib.

Cell necrosis induced by Ib. We next investigated the possible mechanisms responsible for the rapid cell death caused by Ib. Incubation of A431 cells with Ib (250 ng/ml) failed to induce DNA ladder fragmentation, a hallmark of apoptosis, even after incubation for up to 240 min (Fig. 4A). As a positive control, DNA fragmentation was detected when A431 cells were incubated for longer periods of time (24 h) with 10 nM staurosporine, a well-known inducer of apoptosis (Fig. 4A). No induction of apoptotic caspase 3 was detected in Ib-treated cells (data not shown). Moreover, preincubating the cells with 20 μM Z-VAD-FMK, a broad-spectrum caspase inhibitor, and 3-methyladenine, an autophagy inhibitor, did not protect against the rapid loss of cell viability caused by the toxin, as assessed by MTS assay (data not shown). Loss of plasma membrane integrity leading to increased permeability to cationic dyes such as propidium iodide (PI) was found to be characteristic of necrosis, or the so-called "necrotic stage" of apoptosis (22). Therefore, the entry of PI into cells treated with Ib was monitored. As shown in Fig. 4B, Ib induced the entry of PI into cells in a time-dependent manner. PI entry into MDCK cells with Ib was not observed. The results supported the idea that Ib causes cell necrosis. Next, the cell damage induced by Ib was

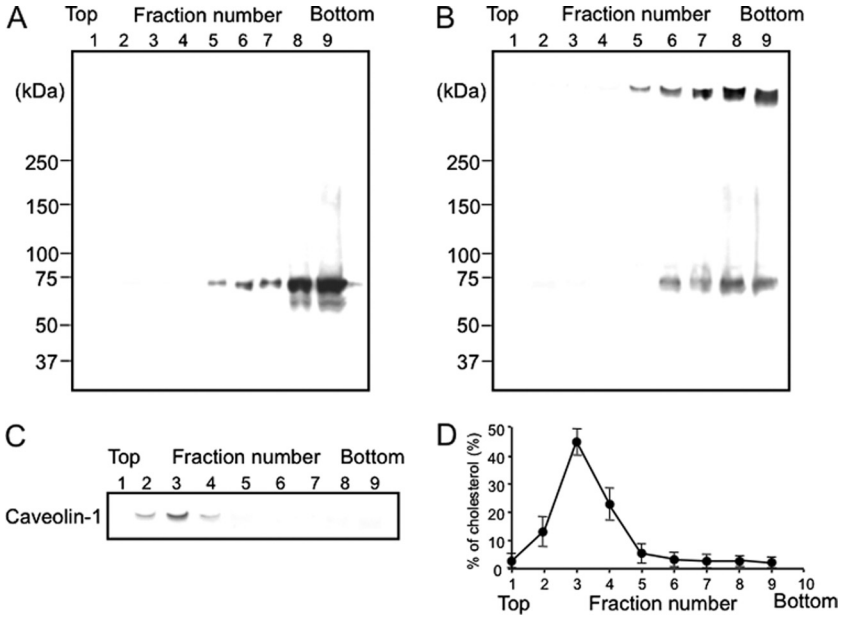

FIG. 3. Sucrose density gradient analysis of Ib-bound A431 cells. A431 cells were incubated with Ib (1 μg/ml) in DMEM containing 10% fetal calf serum at 4°C for 1 h and then either analyzed (A) or washed, incubated at 37°C for 30 min, and then analyzed (B). Cells were solubilized in 1% Triton X-100, and detergent-insoluble fractions were floated on a step sucrose gradient. Aliquots of the nine fractions from the gradient were analyzed by Western blot analysis using anti-Ib antibody (A and B) or anti-caveolin-1 antibody (C). (D) The distribution of cholesterol in the sucrose gradient fractions was determined as described in Materials and Methods.

investigated by electron microscopy (Fig. 4C). When A431 cells were incubated with Ib at 37°C, the density of the cytoplasm and the nucleus decreased. In addition, swelling of the nucleus and small vacuoles were observed. Consistent with above results, ultrastructural studies revealed that A431 cells treated with Ib display the morphological changes characteristic of necrosis.

Ib caused a rapid decrease in the ATP content of A431 cells, with almost complete depletion after 30 min, as shown in Fig. 1. We next tested whether Ib-induced ATP depletion altered mitochondrial permeability. Mitochondria were visualized using MitoTracker red, a mitochondrion-specific dye that accumulates in a membrane potential-dependent way. The staining of mitochondria in control cells was homogenous, indicative of actively respiring mitochondria; the mitochondria appeared to be almost evenly distributed within the cell, particularly around the nuclei (Fig. 5A). On the other hand, mitochondria in cells treated with Ib for 15 min revealed a striking decrease in fluorescent intensity (Fig. 5A). Next, we used A431 cells expressing Mitochondria-GFP (Mito-GFP). In this experiment, GFP with a mitochondrion-targeting signal (Mito-GFP) was used as a marker for mitochondria. As shown in Fig. 5B, we investigated whether Ib causes the release of cytochrome *c* from the mitochondria to the cytosol. In control cells, cytochrome *c* immunoreactivity was not revealed in the cytoplasm. On the other hand, Ib induced the release of cytochrome *c* from mitochondria in the cytoplasm of cells within 30 min. It has been reported that the proapoptotic Bcl-2-family proteins, such as Bax, induce mitochondrial membrane permeabilization and cytoplasmic release of cytochrome *c* (1). We therefore examined whether the Ib-induced release of cytochrome *c* from mitochondria involved the activation of Bax. It had been reported that activated Bax was associated with intracellular membranes, principally the mitochondrial outer membrane (29). We evaluated the subcellular distribution of activated Bax in Ib-treated A431 cells expressing Mito-GFP using active-form-specific anti-Bax antibodies and confocal microscopy. As shown in Fig. 5B, activated Bax in Ib-treated A431 cells was colocalized to mitochondria within 30 min. In addition, we also observed the activation of Bak by Ib using conformational-specific anti-Bax antibodies (Fig. 5B), indicating that activated Bak, another Bcl-2 homolog, is also colocalized to mitochondria.

DISCUSSION

In the present study, we demonstrated that Ib (i) shows cytotoxicity in A431 and A549 cells, (ii) binds to nonlipid rafts and forms an oligomer, and (iii) causes a rapid necrosis.

It has been reported that Ib possesses no cytotoxic activity (3, 18, 20). We found that Ib binds to Vero cells, forming homo-oligomers to create ion-permeable channels, but the oligomers did not induce cytotoxicity (11). The finding suggests that Ib forms channels comprising heptamers or hexamers in the membrane (functional oligomers) and that the Ib oligomer is inserted into the endosomal membrane (11). Knapp et al. (8) reported that Ib was able to induce the formation of small ion-permeable channels in artificial lipid bilayer membranes. The putative channel-forming domain in Ib plays a role in the formation of channels (8). Richard et al. (16) reported that Ib alone applied apically or basolaterally induced a slow decrease in the transepithelial resistance (TER) of Caco-2 cell monolayers and that Ib was transcytosed on the opposite cell surface. In the present study, Ib induced marked swelling, ATP deple-

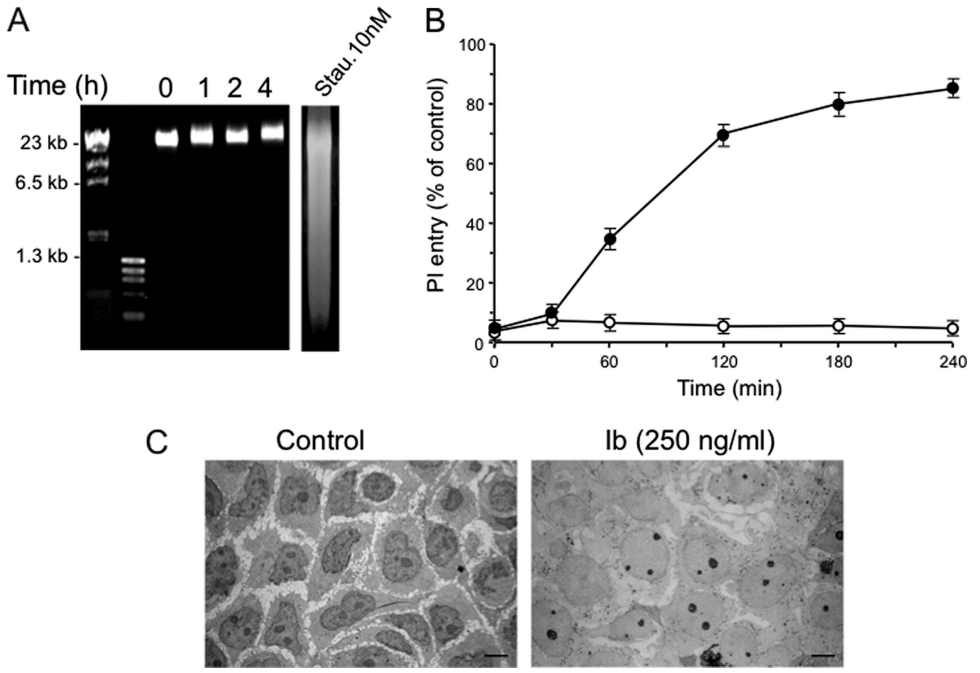

FIG. 4. Effect of Ib on entry of propidium iodide (PI), DNA fragmentation, and ultrastructural change. (A) Nuclear DNA from untreated A431 cells (lane 0) and cells exposed to Ib (250 ng/ml) at 37°C for 1 to 4 h (lanes 1, 2, and 4) was analyzed by agarose gel electrophoresis. As a positive control, A431 cells were treated with 10 nM staurosporine (Stau.) for 24 h. (B) Cells were incubated with Ib (250 ng/ml) and PI (5 μg/ml) at 37°C for the periods indicated. Control cells (100%) were treated at 37°C for 30 min with 0.2% Triton X-100. Data are means ± standard deviations for four independent experiments. Symbols: ●, A431; ○, MDCK. (C) Ultrastructural changes caused by Ib. A431 cells were incubated without or with Ib (250 ng/ml) at 37°C for 30 min. Cells were then processed for transmission electron microscopy as described in Materials and Methods. Bar, 10 μm.

tion, and cell death among sensitive cells. Since no cell line has been reported to be sensitive to date, the discovery that A431 and A549 cells are sensitive to Ib is a novel finding and may resolve the role of Ib in pathogenicity.

We reported previously that Ib binds to a receptor in membranes of MDCK cells and then moves to lipid rafts in the membranes and that the oligomer of Ib formed in the rafts is internalized (13). Here, we also showed that Ib enters MDCK cells via endocytosis. On the other hand, the Ib monomer formed oligomers on nonlipid rafts in membranes of sensitive A431 cells. Moreover, Ib was located on the cell surface during the intoxication process at 37°C. Husmann et al. (7) reported that *S. aureus* alpha-toxin persistence in plasma membranes was cell type dependent and that uptake of the toxin correlated with the ability to survive attack by the pore former. Therefore, the ability of a cell type to survive membrane perforation by Ib appeared to depend on its ability to internalize Ib. The present data indicate that internalization of Ib is required for cellular survival and suggest a role for endocytosis as an innate cellular defense mechanism against small membrane pores.

We found that Ib induced cell swelling and cell death. Ib induced activation of the proapoptotic Bcl homologues Bax and Bak, known to cause mitochondrial membrane permeabilization, and cytoplasmic release of cytochrome *c*. However, no expression of the apoptotic enzyme caspase 3 was detected in Ib-treated cells. Preincubating the cells with Z-VAD-FMK, a broad-spectrum caspase inhibitor, did not protect against the rapid loss of viability caused by Ib. Moreover, Ib did not induce DNA fragmentation. These results indicate that even if Ib induced activation of Bak and Bax, the cell death mechanism caused by Ib did not result from the activation of a caspase-dependent apoptotic process. Ib caused the entry of PI and rapid cellular depletion of ATP, which is one of the early signals leading to necrosis. The Ib-dependent increase in permeability by PI correlated with the loss of viability, further supporting the idea that Ib caused necrosis. Moreover, ATP levels decreased to below 90% of normal values within 60 min of Ib treatment, at which point cells are considered necrotic, since there is no longer sufficient ATP to maintain energy-dependent apoptotic pathways. Ib treatment also results in the permeabilization of mitochondrial membranes, reflected by the release of cytochrome *c* into the cytoplasm and the loss of MitoTracker staining. Mitochondrial dysfunction was a significant contributor to cytotoxicity; indeed, severe ATP depletion could be sufficient to cause cell death. These results suggest that Ib induces the mitochondrial dysfunction, which in turn appears to contribute to ATP depletion. The proapoptotic Bcl-2 homologs Bax and Bak are both critical regulators of mitochondrial membrane permeabilization, with partially redundant functions (1). Bax is a cytosolic, monomeric protein in nonapoptotic cells; during apoptosis, it undergoes conformational changes near the amino and carboxyl termini to expose the functionally crucial Bcl-2 homology domain 3 and translocates to the mitochondrial outer membrane (29). Bak is largely associated with the mitochondrial outer membrane and endoplasmic reticulum, even in healthy cells; it, too, changes conformation in response to apoptotic stimuli. Activated Bax and Bak undergo homo-oligomerization and may participate in the

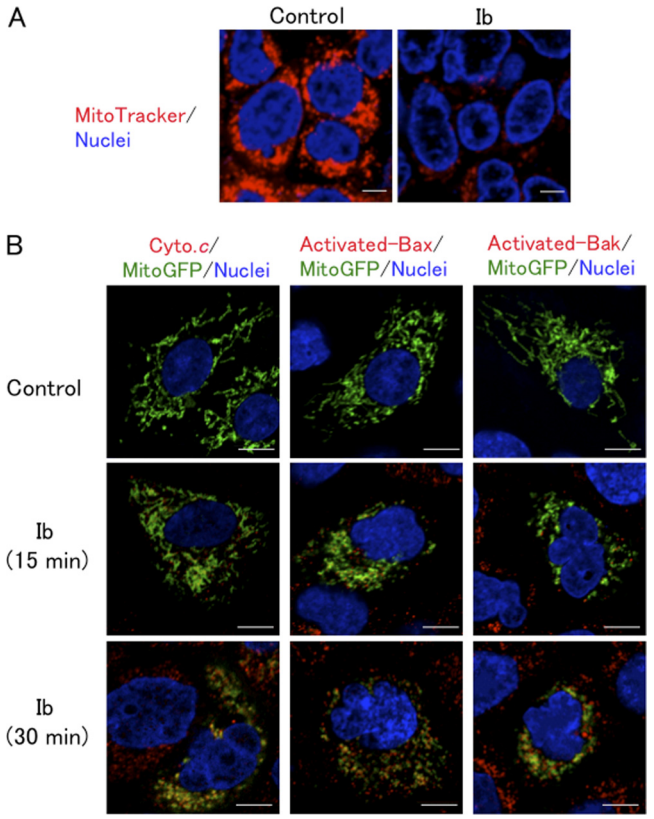

FIG. 5. Ib induces mitochondrial dysfunction. (A) A431 cells prestained with MitoTracker red and Hoechst 33342 were incubated with Ib (250 ng/ml) at 37°C for 15 min and observed under a confocal microscope. (B) A431 cells transfected with Mito-GFP were incubated with Ib (250 ng/ml) at 37°C for the periods indicated. Cells were then fixed, permeabilized, and stained with anti-cytochrome *c* antibody, active-form-specific anti-Bax antibody, or active-form-specific anti-Bak antibody. Nuclei were stained with DAPI. Cells were observed by confocal microscope. The images are representative of four experiments. Bar, 5 μm.

formation of a large mitochondrial transition pore complex that facilitates cytochrome *c* release (1, 29). Here, we demonstrated that Bax was activated and localized to mitochondria in A431 cells exposed to Ib. In addition to Bax activation in Ib-treated A431 cells, we observed Bak activation by confocal microscopy using conformation-specific anti-Bak antibodies. These results indicate that Ib may utilize both Bax and Bak to induce mitochondrial dysfunction. We found that Ib was associated with plasma membranes even in A431 cells in which cytochrome *c* release had been induced. These results suggested that Ib-induced cytochrome *c* release did not necessarily require direct interaction of Ib with mitochondria; rather, an alternative signaling pathway resulting in Bax and Bak activation appears to be important to the actions of Ib.

C. perfringens type E reportedly causes enterotoxemia in calves and occasionally other young animals (23). Previous works demonstrated the ADP-ribosylating nature of iota toxin, but this toxin's role in the pathogenesis of intestinal infections was still unclear (2, 23). It has been reported that Ib alone decreased the transepithelial resistance (TER) of Caco-2 cell monolayers through the formation of pores resulting from the membrane insertion of Ib oligomers (16) and that the Ib oligomer in cell membranes generates ion-permeable pores (8, 13). In the present study, we demonstrated that Ib alone induced cytotoxicity in particular types of cells. Based on these findings, A431 cells could be a useful model for improving our understanding of the mechanisms involved in the cytotoxicity of Ib.

In summary, we showed that Ib causes rapid depletion of ATP and necrosis in A431 and A549 cells. These cells therefore offer an attractive new cell system that could be used to analyze the cytotoxic action of Ib.

ACKNOWLEDGMENTS

We thank A. Kanbayashi and R. Tashiro for technical assistance.

This work was supported by a grant-in-aid for Scientific Research from the Ministry of Education, Culture, Sports, Science, and Technology of Japan, MEXT.SENRYAKU, 2010.

REFERENCES

1. **Adams, J. M.** 2003. Ways of dying: multiple pathways to apoptosis. Genes Dev. **17:**2481–2495.
2. **Aktories, K., and A. Wegner.** 1989. ADP-ribosylation of actin by clostridial toxins. J. Cell Biol. **109:**1385–1387.
3. **Barth, H., K. Aktories, M. R. Popoff, and B. G. Stiles.** 2004. Binary bacterial toxins: biochemistry, biology, and applications of common *Clostridium* and *Bacillus* proteins. Microbiol. Mol. Biol. Rev. **68:**373–402.
4. **Blöcker, D., J. Behlke, K. Aktories, and H. Barth.** 2001. Cellular uptake of the *Clostridium perfringens* binary iota-toxin. Infect. Immun. **69:**2980–2987.
5. **Gibert, M., et al.** 2007. Differential requirement for the translocation of clostridial binary toxins: iota toxin requires a membrane potential gradient. FEBS Lett. **581:**1287–1296.
6. **Hale, M. L., J. C. Marvaud, M. R. Popoff, and B. G. Stiles.** 2004. Detergent-resistant membrane microdomains facilitate Ib oligomer formation and biological activity of *Clostridium perfringens* iota-toxin. Infect. Immun. **72:**2186–2193.
7. **Husmann, M., et al.** 2009. Elimination of a bacterial pore-forming toxin by sequential endocytosis and exocytosis. FEBS Lett. **583:**337–344.
8. **Knapp, O., R. Benz, M. Gibert, J. C. Marvaud, and M. R. Popoff.** 2002. Interaction of *Clostridium perfringens* iota-toxin with lipid bilayer membranes. Demonstration of channel formation by the activated binding component Ib and channel block by the enzyme component Ia. J. Biol. Chem. **277:**6143–6152.
9. **Kobayashi, K., et al.** 2008. Role of Ca^{2+}-binding motif in cytotoxicity induced by *Clostridium perfringens* iota-toxin. Microb. Pathog. **44:**265–270.
10. **Marvaud, J. C., et al.** 2001. *Clostridium perfringens* iota-toxin: mapping of receptor binding and Ia docking domains on Ib. Infect. Immun. **69:**2435–2441.
11. **Nagahama, M., K. Nagayasu, K. Kobayashi, and J. Sakurai.** 2002. Binding component of *Clostridium perfringens* iota-toxin induces endocytosis in Vero cells. Infect. Immun. **70:**1909–1914.
12. **Nagahama, M., S. Hayashi, S. Morimitsu, and J. Sakurai.** 2003. Biological activities and pore formation of *Clostridium perfringens* beta toxin in HL 60 cells. J. Biol. Chem. **278:**36934–36941.
13. **Nagahama, M., et al.** 2004. Binding and internalization of *Clostridium perfringens* iota-toxin in lipid rafts. Infect. Immun. **72:**3267–3275.
14. **Perelle, S., M. Gibert, P. Boquet, and M. R. Popoff.** 1993. Characterization of *Clostridium perfringens* iota-toxin genes and expression in *Escherichia coli.* Infect. Immun. **61:**5147–5156. (Author's correction, **63:**4967, 1995.)
15. **Petosa, C., R. J. Collier, K. R. Klimpel, S. H. Leppla, and R. C. Liddington.** 1997. Crystal structure of the anthrax toxin protective antigen. Nature **385:**833–838.
16. **Richard, J. F., et al.** 2002. Transcytosis of iota-toxin across polarized CaCo-2 cells. Mol. Microbiol. **43:**907–917.
17. **Sakurai, J., and K. Kobayashi.** 1995. Lethal and dermonecrotic activities of *Clostridium perfringens* iota toxin: biological activities induced by cooperation of two nonlinked components. Microbiol. Immunol. **39:**249–253.
18. **Sakurai, J., M. Nagahama, and S. Ochi.** 1997. Major toxins of *Clostridium perfringens*. J. Toxicol. Toxin Rev. **16:**195–214.
19. **Sakurai, J., M. Nagahama, J. Hisatsune, N. Katunuma, and H. Tsuge.** 2003. *Clostridium perfringens* iota-toxin, ADP-ribosyltransferase: structure and mechanism of action. Adv. Enzyme Regul. **43:**361–377.
20. **Sakurai, J., M. Nagahama, M. Oda, H. Tsuge, and K. Kobayashi.** 2009. *Clostridium perfringens* iota-toxins: structure and function. Toxins **1:**208–228.
21. **Schleberger, C., H. Hochmann, H. Barth, K. Aktories, and G. E. Schulz.** 2006. Structure and action of the binary C2 toxin from *Clostridium botulinum*. J. Mol. Biol. **364:**705–715.

22. **Smolewski, P., J. Grabarek, H. D. Halicka, and Z. Darzynkiewicz.** 2002. Assay of caspase activation in situ combined with probing plasma membrane integrity to detect three distinct stages of apoptosis. J. Immunol. Methods **265:**111–121.
23. **Songer, J. G.** 1996. Clostridial enteric diseases of domestic animals. Clin. Microbiol. Rev. **9:**216–234.
24. **Stiles, B. G., M. L. Hale, J. C. Marvaud, and M. R. Popoff.** 2000. *Clostridium perfringens* iota-toxin: binding studies and characterization of cell surface receptor by fluorescence-activated cytometry. Infect. Immun. **68:**3475–3484.
25. **Stiles, B. G., M. L. Hale, J. C. Marvaud, and M. R. Popoff.** 2002. *Clostridium perfringens* iota toxin: characterization of the cell-associated complex. Biochem. J. **367:**801–808.
26. **Tone, S., et al.** 2007. Three distinct stages of apoptotic nuclear condensation revealed by time-lapse imaging, biochemical and electron microscopy analysis of cell-free apoptosis. Exp. Cell Res. **313:**3635–3644.
27. **Tsuge, H., et al.** 2003. Crystal structure and site-directed mutagenesis of enzymatic components from *Clostridium perfringens* iota-toxin. J. Mol. Biol. **325:**471–483.
28. **Tsuge, H., et al.** 2008. Structural basis of actin recognition and arginine ADP-ribosylation by *Clostridium perfringens* iota-toxin. Proc. Natl. Acad. Sci. U. S. A. **105:**7399–7404.
29. **Yamasaki, E., et al.** 2006. *Helicobacter pylori* vacuolating cytotoxin induces activation of the proapoptotic proteins Bax and Bak, leading to cytochrome *c* release and cell death, independent of vacuolation. J. Biol. Chem. **281:** 11250–11259.

Editor: J. B. Bliska